A Thesis on

DESIGN AND FABRICATION OF AN EXPERIMENTAL SET-UP FOR AC SUSCEPTIBILITY MEASUREMENT

Submitted for the Award of the Degree of

Master of Science

By

RAKHEE SHARMA
409PH2107

Under the academic autonomy

National Institute of Technology, Rourkela

Under the Guidance of

Dr. Prakash Nath Vishwakarma

Department of Physics

National Institute of Technology

Rourkela-769008

2009-2011

CERTIFICATE

This is to certify that the thesis entitled "Design & Fabrication of an Experimental Set-up for Susceptibility Measurement" submitted by Rakhee Sharma in partial fulfillment of the requirements for the award of degree of Master of Science in Physics at National Institute of Technology, Rourkela is an authentic work carried out by her under our supervision. To the best of my knowledge, the matter embodied in this thesis has not been submitted by any other university/ Institute for the award of any degree or diploma.

Date -

Dr. Prakash Nath Vishwakarma
Department of Physics
National Institute of Technology
Rourkela.

Department of Physics
National Institute of Technology
Rourkela – 769008 (Orissa)

DECLARATION

I hereby declare that the project work entitled ***"Design & Fabrication of an Experimental Set-up for ac Susceptibility Measurement"*** submitted to NIT,Rourkela, is a record of an original work done by me under the guidance of **Dr. Prakash Nath Vishwakarma**,Faculty Member of NIT,Rourkela and this project work has not performed the basis for the award of any Degree or Diploma/ Associate-ship/Fellowship and similar project if any.

Date -

Rakhee Sharma.
Department of Physics.
NIT, Rourkela.

ACKNOWLEDGEMENT

First of all my heartful thanks to almighty for reasons too numerous to mention.

My sincere gratitude to my mentor ***Dr.P.N.Vishwakarma*** for guiding me all through the course of my project. I truly thank him for his esteemed encouragement from the beginning to the end of the project.

I am grateful to the **Department of Physics , N.I.T Rourkela** for providing all the required facilities.

I would also like to acknowledge Mr. Achyuta Kumar Biswal for helping a great deal in this work.

I express my gratitude towards Miss Jashashree Ray for the help she extended to me. I thank Miss Sanghamitra Acharya for her support and also all PhD scholar who are related in the completion of my work.

I also acknowledge the Central Workshop for giving me their facility in fabricating my setup. I am thankful to The Department of Metallurgy for letting me avail their XRD Characterization technique.

I am extremely grateful to my parents for support and blessings.

I heartily thank my project partner Debjani Banerjee for her co-operation.

In particular, I would thank my friends who by any way stimulated me in the completion of my work.

Rakhee Sharma.

Department of Physics.

N.I.T Rourkela.

DEDICATED TO MY PARENTS...

CONTENTS

ABSTRACT

In this project , an experimental set up for ac susceptibility measurement, is designed and fabricated . The setup comprises of, primary coil, secondary coil and sample holder. The basic principle of the setup is “mutual induction”. Copper wire winding is done over secondary and primary coil uniformly. When current passed, the coil gets magnetised which in turn magnetizes the sample. The setup is fabricated both for room temperature and high temperature susceptibility measurement. A sample is prepared whose susceptibility is to be measured. Cobalt Ferrite, a ferrimagnetic sample is chosen for the purpose. The sample is made by auto combustion sol-gel method. XRD characterization was carried out. Measurements were taken at high temperature and susceptibility versus temperature graphs were plotted. The graphs are in good agreement with the standard CFO graphs.

Chapter 1

INTRODUCTION

In the modern concept all materials like metals, semiconductors and insulators are said to exhibit magnetism, though of different nature. When a solid is placed in a magnetic field it gets magnetised. By magnetised, we mean the magnetic dipoles inside the material gets align along the direction of magnetic field. The moment carried by the magnetic dipoles are called magnetic moment. Magnetic moment per unit volume developed inside a solid is called magnetisation and is denoted by 'M'. The effect of magnetic field on a material may be expressed by the relation,

SI	CGS
$B = \mu_0 (H + M)$	$B = H + 4\pi M$
$\frac{B}{H} = \mu_0 \left(1 + \frac{M}{H}\right) \quad \boxed{\Rightarrow \mu = \mu_0 (1 + \chi)}$	$\frac{B}{H} = 1 + \frac{4\pi M}{H} \quad \boxed{\Rightarrow \mu = 1 + 4\pi\chi}$

Where, 'B' is magnetic flux density or magnetic induction and is the measure of magnetic lines of force passing per unit area, H is the applied magnetic field and M is the magnetization. $\mu = B/H$ is the magnetic permeability and $\chi = M/H$ is the *magnetic susceptibility* of the material. The parameter χ is a measure of the quality of the magnetic material and is defined as the magnetisation produced per unit applied magnetic field. In isotropic medium, χ is a scalar quantity. Generally, χ is a dimensionless quantity. Quite frequently susceptibility is defined with respect to unit volume or unit mass or unit molar of substance. If the susceptibility is measured per unit mole of substance, then it is termed as *molar susceptibility* and is written as χ_{mol}. Similarly, for volume susceptibility $\chi_v = M/H$,

mass susceptibility $\chi_{mass} = \chi_v/\rho$, and molar susceptibility $\chi_{mol} = M\,\chi_{mass} = M\,\chi_v/\rho$ where ρ is the density. The magnitude and sign of susceptibility vary with the type of magnetism, and hence characterises the various magnetic materials. Although B, H, and M must necessarily have the same units, it is customarily to denote in CGS (SI) units, 'B' in gauss (G) or tesla (T), 'H' in Oersted(Oe) = A/m and 'M' in erg/Oe cm^3 or emu/cm^3 (A/m) **[1]**.

1.1 MAGNETIC BEHAVIOUR OF MATERIALS:

According to the modern theory, magnetism in solids arises due to orbital and spin motion of electrons as well as spin of the nuclei. The motion of electron is equivalent to an electric current which produces the magnetic effects. The major contribution comes from the spin of unpaired valance electrons which produces permanent electronic magnetic moments. **[2]**. A number of such magnetic moments may align themselves to generate a net non-zero magnetic moment, with or without the application of magnetic field. Thus the nature of magnetization produced depends on the number of unpaired valence electrons present in the atoms of the solid and on the relative orientations of the neighbouring magnetic moments.

The magnetism in solids has been classified into the following five categories:

1. Diamagnetism
2. Paramagnetism
3. Ferromagnetism
4. Antiferromagnetism
5. Ferrimagnetism

Diamagnetism is a very weak effect exhibited in solids, where magnetic moments are always directed opposite to the applied magnetic field. The existence of a small non-zero magnetic moment in these materials is attributed to the orbital motion of the electrons. Example -He, Ne, Ar, Xe, YBCO, NaCl, etc.

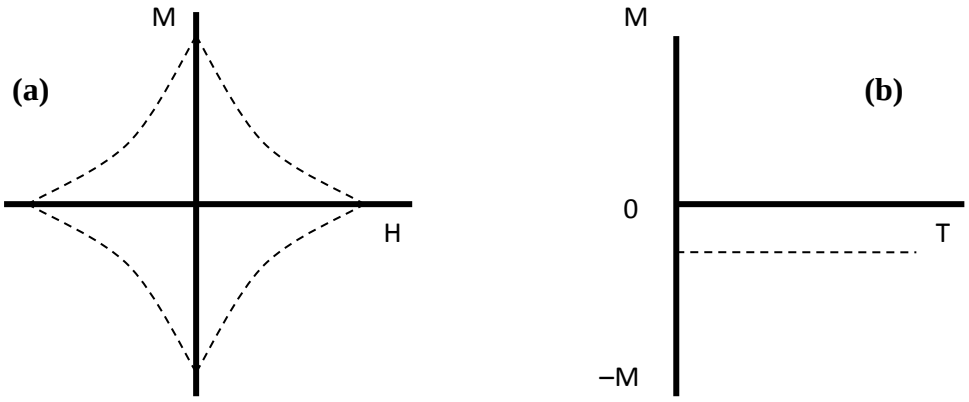

Figure1.1 shows the (a) M-H curve (superconductor) and (b) M vs T plot for diamagnetic materials. Susceptibility is negative and temperature independent for diamagnets. **[2]**

Paramagnetism arises due to the presence of permanent atomic or electronic magnetic moment. It is also a weak effect but unlike diamagnetism, the magnetic moment is aligned in the direction of the field. Example Pt, Na, $MnSO_4$, $CoCl_2$ etc.

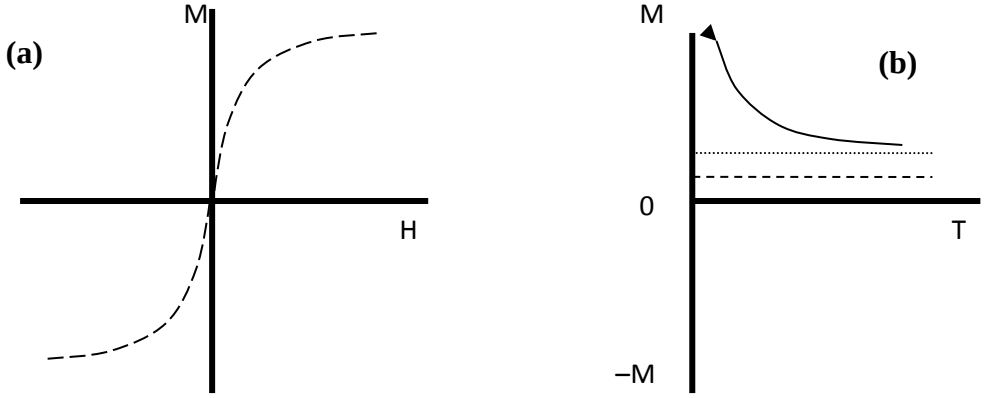

Figure-1.2 shows the (a) M-H curve and (b) shows M-T response of paramagnetic materials. The solid line is for Langevin (free spin) paramagnetism the dotted line is for Van Vleck paramagnetism and dashed line is for Pauli paramagnetism(metals).At normal temperature, in moderate field the magnetization is small. This results in temperature dependent susceptibility known as Curie law. **[2]**

Ferromagnetism is a very strong effect and arises when the adjacent magnetic moment align themselves in the same direction with in a small region called domains. The domains aligned in the applied magnetic field direction resulting an enhancement of total magnetization value. Example- Fe, Mn, Ni, CrO_2, MnSb etc.

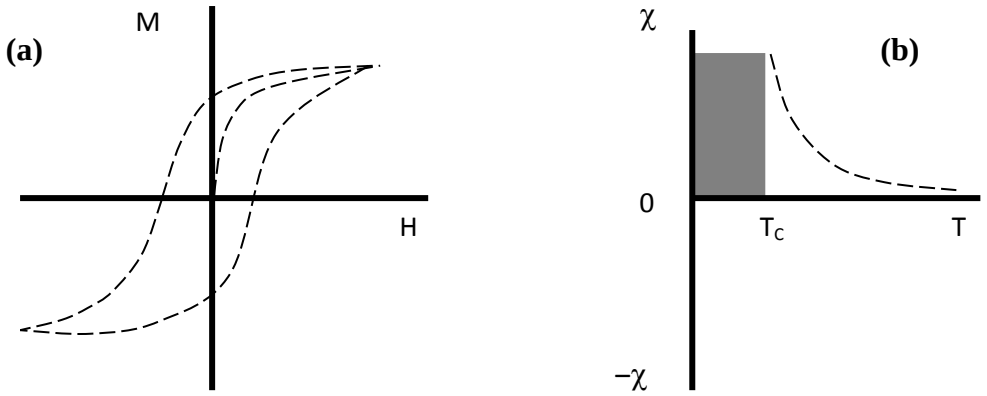

Figure 1.3 shows (a) M-H loop (b) M-T response of ferromagnetic materials. Below curie temperature (T_c) the material is ferromagnetic and above T_c the material behaves as paramagnet. This results in temperature dependent susceptibility known as Curie Weiss law.**[2]**

In *antiferromagnetism* the adjacent magnetic moments are equal and opposite to each other, and hence complete cancellation of moments take place. Example- NiO, MnO, $FeCl_2$, etc.

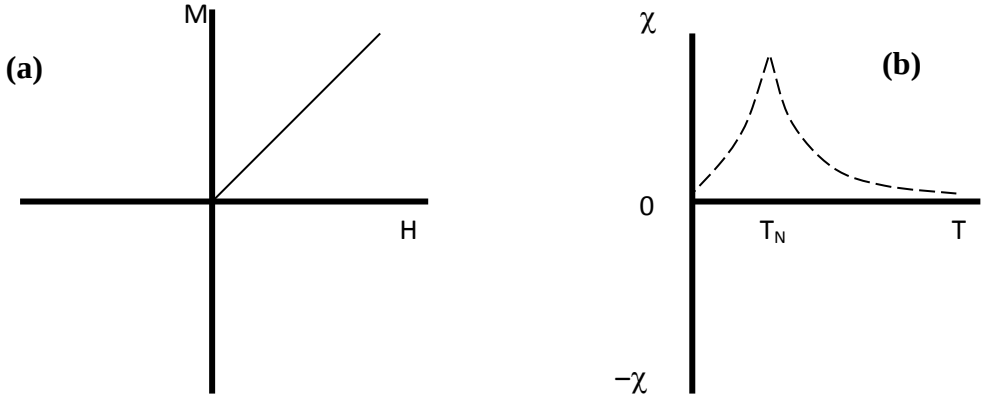

Figure-1.4 shows (a) M-H curve and (b) M-T response of antiferromagnets , Below Neel temperature(T_N) the material is antiferromagnetic and above T_N it is paramagnetic.**[2]**

Ferrimagnetism is similar to antiferromagnetism but except that adjacent moments are unequal in magnitude and hence complete cancellation of moment does not takes place. Example, Fe_3O_4, $MgAl_2O_4$, etc.

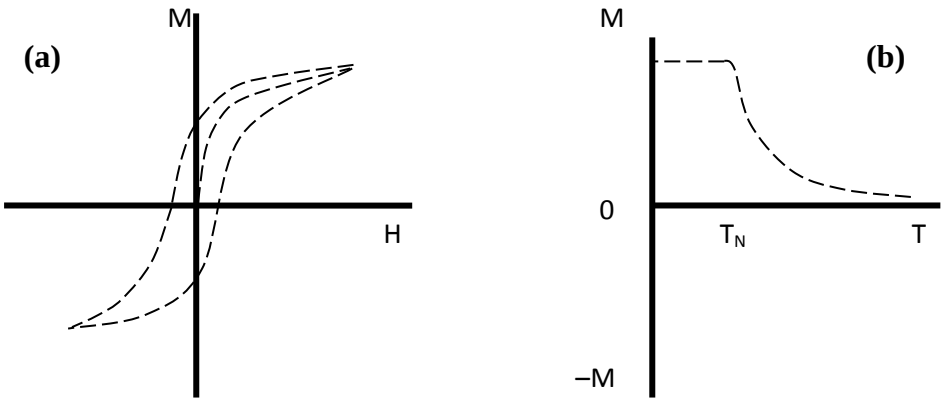

***Figure 1.5 shows the (a) M-H loop and (b) M-T response of ferrimagnetic material. Below Neel temperature(T_N) the material is antiferromagnetic and above T_N it is paramagnetic.*[2]**

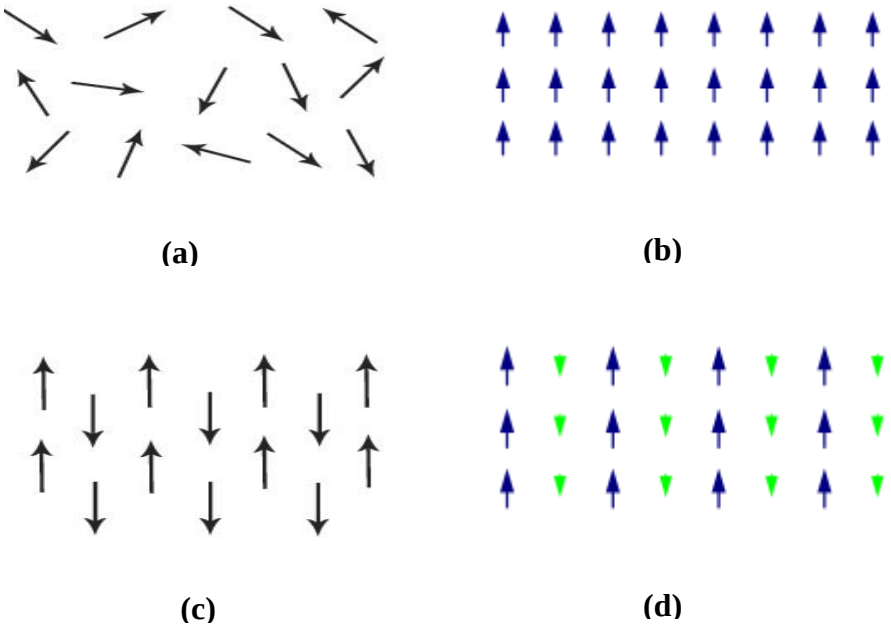

Figure-1.6 shows the magnetic dipole alignment of (a) paramagnets, (b) ferromagnets, (c) antiferromagnets and (d) ferrimagnets respectively.

Since susceptibility is the essential physical parameter, for understanding various magnetic materials. It is relevant to study the measurement of susceptibility.

1.2 SUSCEPTIBILITY MEASUREMENTS

The methods followed by the researchers to measure the susceptibility, are discussed below.

(I) EXTRACTION METHOD:

The basic principle on which this method is based on is the flux change in the search coil when the specimen is removed (or extracted) from the coil, or when the specimen and the search coil together are extracted from the field **[1]**. The total flux through the search coil, when the solenoid is producing a field is

$$\Phi_1 = BA = (H + 4\pi M)A = (H_a - H_d + 4\pi M)A = (H_a - N_d M + 4\pi M)A \qquad \text{(CGS)}$$

$$\Phi_1 = BA = \mu_0(H + M)A = \mu_0(H_a - H_d + M)A = \mu_0(H_a - N_d M + M)A \qquad \text{(SI)}$$

A is the specimen or search coil area. (Both are assumed equal and air flux correction is omitted). H_d is the demagnetizing field ($H_d = N_d M$).

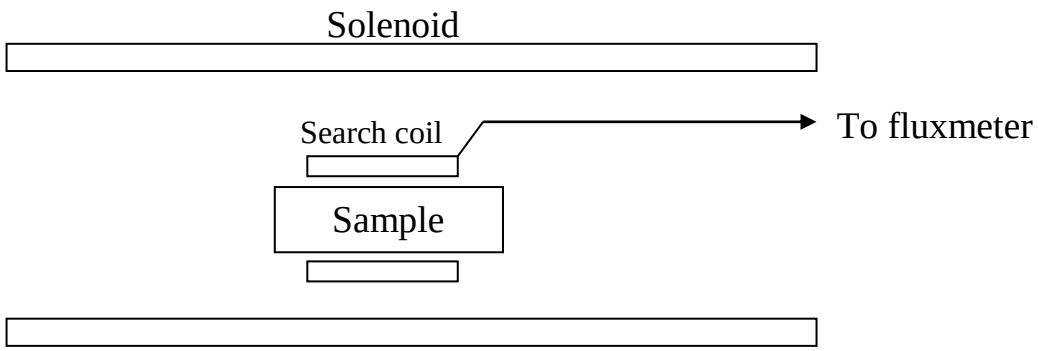

Figure-1.7 shows the arrangement for measuring a rod sample in a magnetizing solenoid.**[1]**

If the specimen is suddenly removed from the search coil, the flux through the coil becomes

$\Phi_2 = H_a A$ (CGS) $\Phi_2 = \mu_0 H_a A$ (SI)

The fluxmeter will therefore record a value proportional to the flux change

$\Phi_1 - \Phi_2 = (4\pi - N_d) MA$ (CGS) $\Phi_1 - \Phi_2 = \mu_0 (1 - N_d) MA$ (SI)

This method measures M directly rather than B. M is measured at particular field strength, rather than as a change in M due to a change in field, and that the flux change in the search coil does not involve H. This fact results in greater sensitivity when M is small compared to H, as it is for weakly magnetic substances. A variation can be can by using two identical coil in series opposition. When the specimen is moved out of one coil and into the other, the measured signal is twice that obtained with a single coil.

(II) VIBRATING SAMPLE MAGNETOMETER:

This is another technique of measurement. It is based on the flux change in a coil when a magnetized sample is vibrated near it **[3]**. The sample, commonly a small disk, is attached to the end of a nonmagnetic rod, the other end of which is fixed to a loudspeaker cone or to some other kind of mechanical vibrator. The oscillating magnetic field of the moving sample induces an alternating emf in the detection coils, whose magnitude is proportional to the magnetic moment of the sample. The (small) alternating emf is amplified, usually with a lock-in amplifier which is sensitive only to signals at the vibration frequency. Note that the VSM measures the magnetic moment ‘m’ of the sample, and therefore the magnetization M, whereas the fluxmeter method ordinarily measures the flux density B. The VSM is very versatile and sensitive. It may be used for both weakly and strongly magnetic substances.

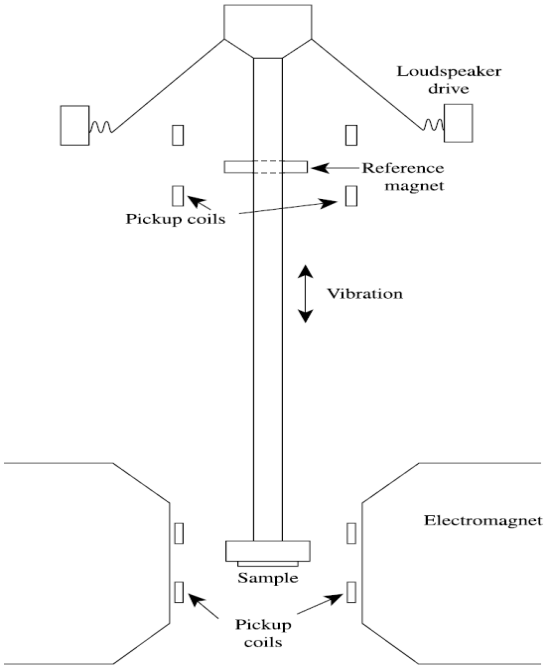

Figure-1.8 shows the schematic diagram of VSM **[1]**

(III) ALTERNATING FIELD GRADIENT MAGNETOMETER (AFGM):

The sensitivity of this method is much higher than VSM. In this method, the sample is mounted at the end of a fiber, and subjected to a fixed dc field plus an alternating field gradient, produced by an appropriate coil pair. The field gradient produces an alternating force on the sample, which causes it to oscillate and flexes the fiber. If the frequency of vibration is tuned to a resonant frequency of the system, the vibration amplitude increases by a factor equal to the quality factor Q of the vibrating system . Piezoelectric crystal is used to generate a voltage proportional to the vibrational amplitude, which in turn is proportional to the sample moment.

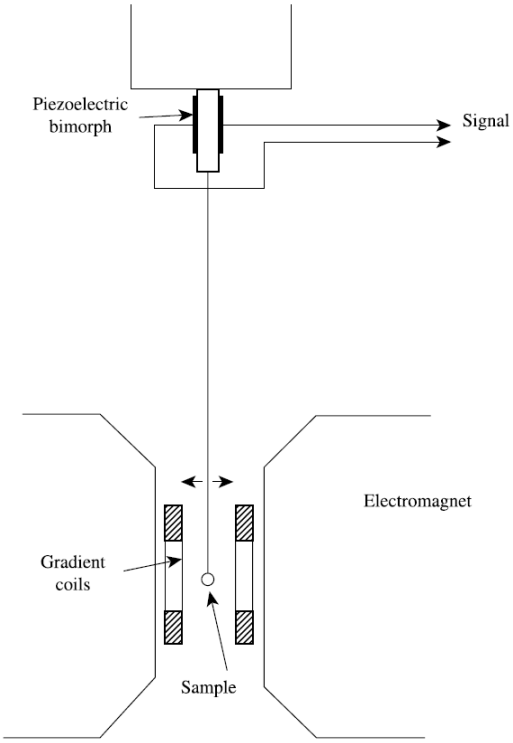

Figure-1.9 shows the schematic diagram of AGFM **[1]**

(IV) SQUID MAGNETOMETER:

The SQUID devices when used as a magnetometer, acts as a very high-sensitivity fluxmeter, in which the integration is performed by counting voltage steps. It is of such high sensitivity that in a working instrument the magnetic field is held exactly constant by a superconducting shield, and the sample is moved slowly through a superconducting pickup coil coupled to the SQUID while flux quanta are counted. Since the SQUID is a superconducting device, it is usually incorporated in a system including a superconducting magnet. Measurements over a range of fields and temperatures are time consuming, and the systems are normally operated unattended, under computer control. The sensitivity of a SQUID magnetometer is more than that of AFGM.

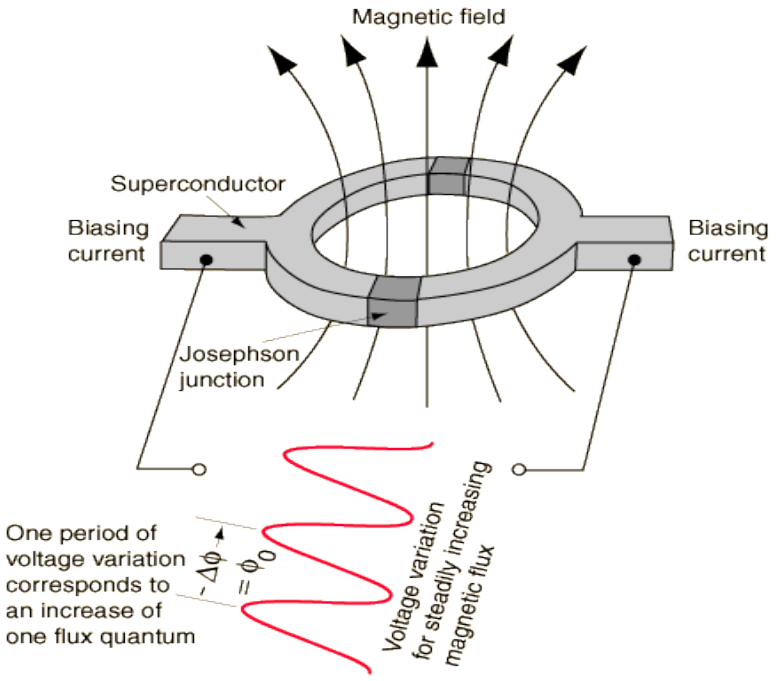

***Figure-1.10 showing a SQUID Magnetometer.*[4]**

From the above measurement methods AC and DC susceptibility can be measured.

1.3 DIFFERENCE BETWEEN AC AND DC SUSCEPTIBILITY

There are mainly two methods used to extract the susceptibility of any material, i.e., ac and dc method. In the dc method, the measured parameter is magnetization, 'M' which may be converted to susceptibility 'χ' using the relation $\chi_{dc} = M / H$, where 'H' is the applied magnetic field. In contrary, the ac method directly gives the susceptibility as $\chi_{ac} = dM / dH$, when an alternating current (ac) is applied. The dc-magnetometer and the ac susceptometer are two entirely different tools that provide different ways of examining magnetic properties. Both these two techniques rely on sensing coils used to measure the variation in the magnetic flux due to magnetic sample.

In a dc magnetization measurement a value for the magnetization 'M' is measured for some applied dc field, H_{dc}. If the sample being measured does not have a permanent magnetic moment, an applied field is required to magnetize the sample. Usually the moment is

measured, as a function of field, and the materials magnetization curve (that is, m or M versus H_{dc}) is determined. A detection coil is used to detect the change in magnetic flux due to the change in magnetic moment of the sample. Since the applied magnetic field is constant, there will be no signal associated with H_{dc} (Faraday's law). The sample flux coupled to the detection coil is made to vary by moving/vibrating the sample.

The dc or static susceptibility is thus given by:

$$\chi_{dc} = M / H_{dc}$$

Though the principle behind dc magnetometer and ac susceptometer is detection of magnetic flux, the main difference lies in how the flux variation is achieved. In ac susceptometer the sample is magnetized by ac magnetic field H_{ac}. The flux produced by the sample placed within a detection coil is sensed by the detection coil. The magnetic moment of the sample generally follows the applied field. The detection circuitry is generally balanced with, a second identical but oppositely wind coil, to null out the flux changes related to H_{ac}. As a result, any experimentally detected change in flux is only due to the changing magnetic moment of the sample (dm) as it responds to the ac field (no sample movement is required to produce an output signal) and not to the moment itself as in dc technique. The ac susceptibility is:

$$\chi_{ac} = dm / VH_{ac} \rightarrow dM/dH$$

Thus, the ac susceptibility is actually the slope (dM/dH) of the magnetization curve (M versus H curve). The ac technique detects changes in the magnetization that lead to dM/dH in the limit of small ac fields, and this is why sometimes referred to as a differential susceptibility. This is the fundamental difference between the ac and dc measurement techniques.

In the dc measurement, the magnetic moment of the sample does not change with time. Thus, a static magnetic measurement is performed. An ac output signal is detected in a VSM, but this signal arises from the periodic movement of the sample, and is not representative of the ac response of the sample itself. In the ac measurement, the moment of the sample is actually changing in response to an applied ac field, allowing the dynamics of the magnetic system to be studied.

Since the actual response of the sample to an applied ac field is measured, the magneto-dynamics can be studied through the complex susceptibility ($\chi'+i\chi''$). The real component χ' represents the component of the susceptibility that is in phase with the applied ac field, while χ'' represent the component that is out of phase. The real component χ' is associated with dispersive magnetic response and the imaginary component χ'' is associated with absorptive components which arise from energy dissipation within the sample.

1.4 WHY AC SUSCEPTIBILITY?

It has a great application in different fields, like spin glass, superparamagnetism, superconductivity etc. A brief discussion is given below.

(I)SPIN-GLASS

Spin-glass behaviour is usually characterized by AC susceptibility **[5].** In a spin-glass, magnetic spins experience random interactions with other magnetic spins, resulting in a state that is highly irreversible and metastable. This spin-glass state is realized below the freezing temperature, and the system is paramagnetic above this temperature. The most studied spin-glass systems are dilute alloys of paramagnets or ferromagnets in nonmagnetic metals. The freezing temperature is determined by measuring χ' vs. temperature, a curve which reveals a cusp at the freezing temperature. The AC susceptibility measurement is particularly important for spin-glasses. Furthermore, the location of the cusp is dependent on the frequency of the AC susceptibility measurement, a feature that is not present in other magnetic systems and therefore confirms the spin-glass phase. Both of these features are evident in AC susceptibility.

(II)SUPERPARAMAGNETISM

AC susceptibility measurements are an important tool in the characterization of small ferromagnetic particles which exhibit superparamagnetism. Superparamagnetism, the theory of which was originally explained by Neel and Brown. In this theory, the particles exhibit single-domain ferromagnetic behaviour below the blocking temperature, T_B, and are superparamagnetic above T_B. In the superparamagnetic state, the moment of each particle freely rotates, so a collection of particles acts like a paramagnet where the constituent

moments are ferromagnetic particles (rather than atomic moments as in a normal paramagnet) **[6]**.

(III)SUPERCONDUCTIVITY

AC susceptibility is the standard tool for determining the physics of superconductors. The Meissner effect, is considered as the fingerprint in superconductivity, but whether it is a surface or bulk phenomenon, can only be determined by ac susceptibility measurements. Moreover, the presence of multi T_C, irreversibility line, critical current density, intergranular and intragranular contribution is also studied by ac susceptibility **[7]**. In the normal state (above the critical temperature), superconductors typically have a small susceptibility. In the fully superconducting state, the sample is a perfect diamagnet and so $\chi' = -1$. Typically, the onset of a significant nonzero χ' is taken as the superconducting transition temperature.

The various applications of ac susceptibility has installed a motivation to design and fabricate an ac susceptometer. For this purpose we have reviewed many literatures, of which one is discussed.

CHAPTER-2

DESIGN AND FABRICATION OF SETUP

2.1 DESIGN OF A TYPICAL SUSCEPTOMETER

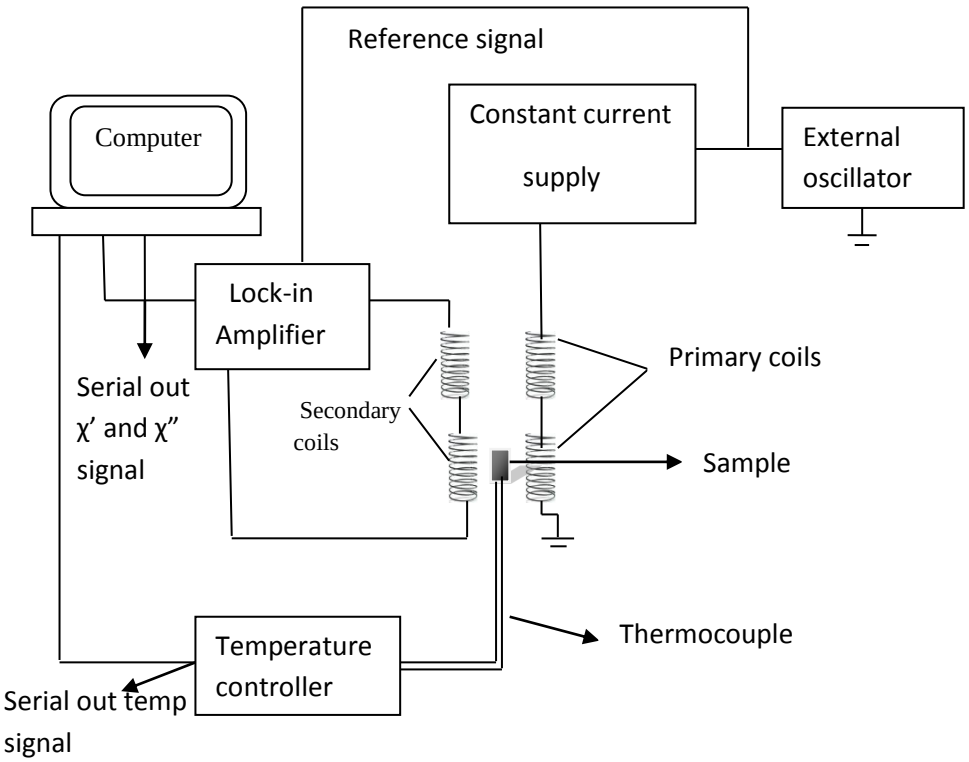

***Figure-2.1 shows the block diagram of a home-made susceptometer.*[8]**

It consists of primary excitation field coil, a secondary pick up coil and a secondary compensation coil. A coated copper wire of 0.1 mm diameter is used for the coil. A four coil system is made which consist of two identical primary excitation field coil of 120 turns each and two identical secondary pick-up coils of 600 turns each. The coils are wound around a hollow "I" shaped cylinder of 1.2 cm in height. An ac magnetic field is generated by the two identical primary coils connected in series. An ac constant current source was coupled to an external oscillator. This permits the measure of ac susceptibility over a broad range of discrete field amplitude, frequency temperature. The pick-up coils were winded beneath the field coils with a shield of low temperature silk thread in tape was used to reduce their capacitive coupling and to achieve a good thermal stability.

The pick-up and reference coils are connected to the differential input of a computer controlled lock in amplifier which is used as an off balance and is coupled to the computer with a stand and serial interface. It is good to coat both the sample and the thermocouple with a thin layer of vacuum grease which acts as a good thermal contact.

2.2 INTRODUCTION TO OUR SETUP

Before finalizing a design, good amount of literature survey is done. A detailed discussion on the principle of measurement using lock-in amplifier is done by M. Nikolo in his paper [9]. An automated ac susceptibility setup is designed by A.Charavorothy et al, but the instead of lock-in they used mutual inductance bridge [10]. Importance of higher orders in the ac susceptibility measurement is discussed by S. Kundu et al, in manganites [11]. M. I. Youssif et.al, discusses the details behind the principle of measurement and the way of extracting the sample susceptibility from the experimental data, taking care of demagnetizing factors [8]. After reviewing these papers, a design was finally prepared. The setup consisted of primary coil, secondary coil and a sample holder. There are two ways to design the setup. The secondary coil can be put inside the primary coil and the primary coil can also be put inside the secondary coil. Our setup's design is based on the former concept because we wanted the secondary coil to be near to the sample for higher induction.

2.3 DESIGN 1

The figure 2.1 shows the cross sectional schematic design of the primary coil, secondary coil and sample holder. Here we made a separate sample holder, as we wanted to wind a small heater wire so that the temperature of the sample may be varied locally. The former material chosen for this purpose is Teflon. All the three parts are machined in Lathe machine as per the specification shown in the fig.2.1. After machining the respective parts were cleaned thoroughly in order to remove oil/grease while machining. The copper winding (150 micron) is done over primary and secondary coils. 1200 turns of copper wire (6 layers) is wound over primary former. The secondary coil is a two coil system and the coiling area is separated by some distance 4mm. It had 500 turns wound in clockwise direction and another 500 turns in counter-clockwise direction. The secondary coil was inserted into the primary coil and the

sample holder was inserted into the secondary pick up coil. A Pt100 temperature sensor is also inserted inside the sample holder, in contact with the sample, for local temperature recording.

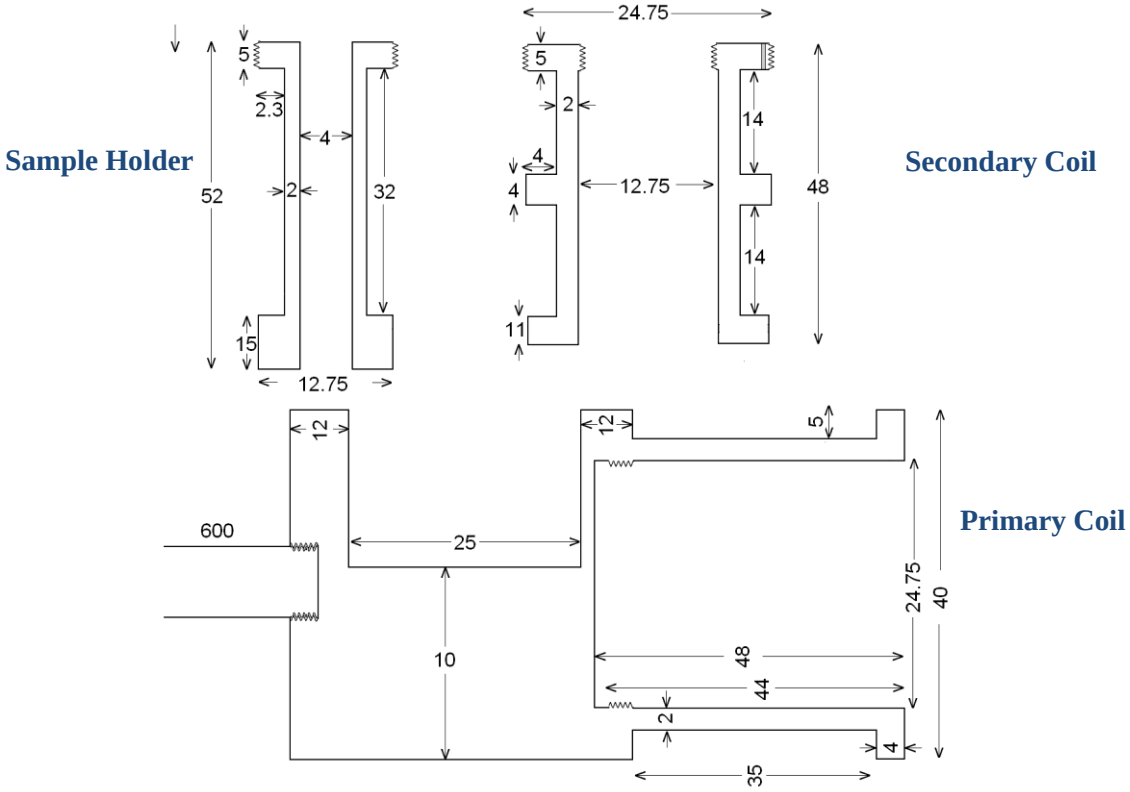

Figure-2.2 shows the dimension (in mm) of the primary ,secondary coil and the sample holder.

The principle of measuring ac susceptibility involves subjecting a sample to a small alternating magnetic field. The flux variation due to the sample is picked up by the secondary coil surrounding the sample and the resulting voltage induced in the coil is detected. This is done by lock-in amplifier which is computer interfaced. This voltage is proportional to the time derivative of the sample's magnetization. Using the concept of mutual induction, the susceptibility χ can be calculated in terms of measurable quantities.

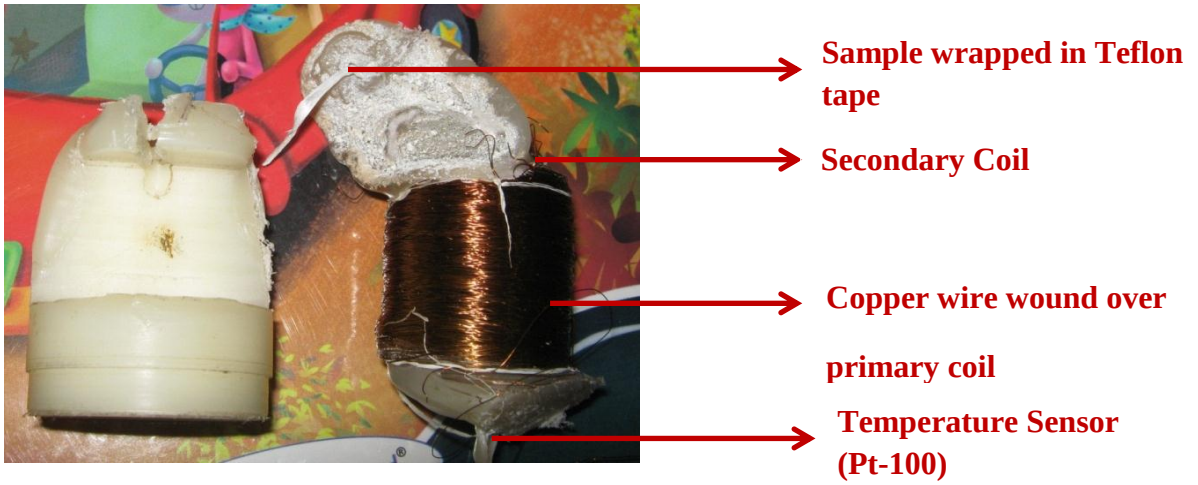

Figure-2.3 shows the assembled first setup which was burnt.

At room temperature the readings were taken appropriately. For high temperature measurement the instrument was inserted into the furnace. When the temperature of furnace reached ~200^{0}C, the setup melted (see fig 2.3). This mishap took place because wrong material was supplied to us by the dealer. In the name of Teflon, some other material was supplied.

2.4 DESIGN 2

After the first mishap, high quality Teflon rod of 1-inch diameter is procured from another vendor. As the diameter of rod was 1-inch, we had to do some alterations in our original design. This setup had primary coil and secondary coil. The sample holder part is omitted here. The no. of copper wire winding on the primary coil was 1200 turns. The secondary coil had 600 turns wound clockwise and 600 turns wound counter-clockwise. The same principle discussed above for ac susceptibility measurement was employed and readings at room temperature and high temperature upto 200^{0}C was recorded.

The sample (pellet form which is cut cylindrically) was rolled over Teflon tape and placed inside the secondary coil. Great care has been given on the miniaturization of the instrument to achieve high sensitivity.

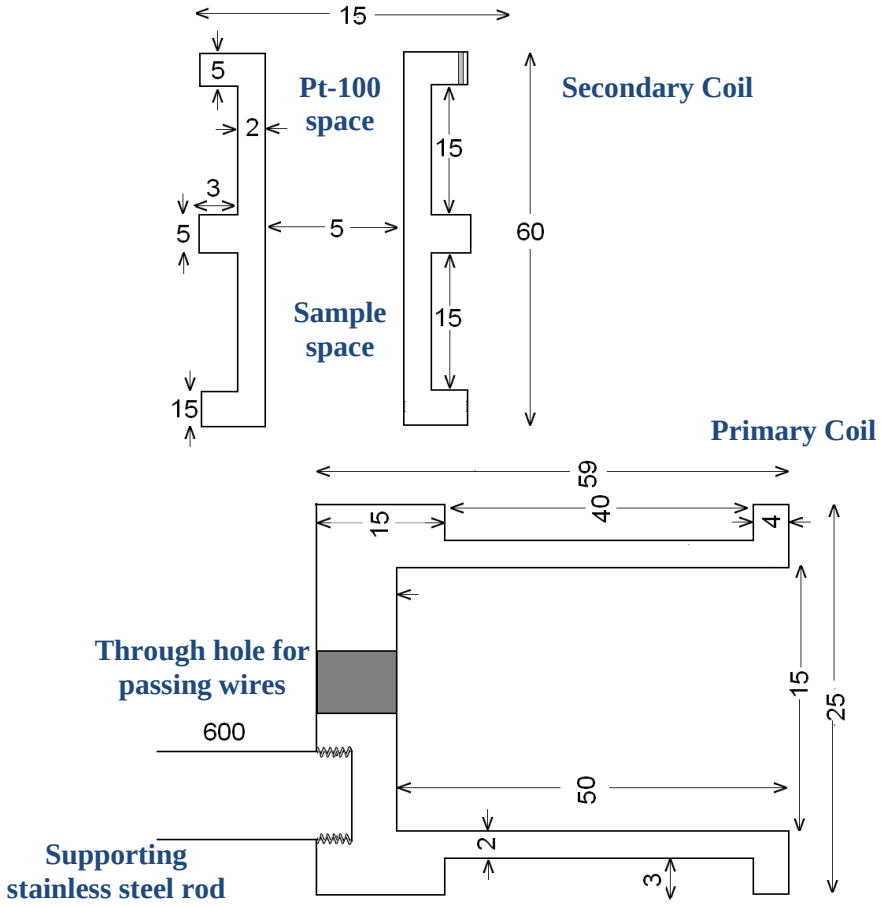

Figure-2.4 shows the schematic diagram of second design

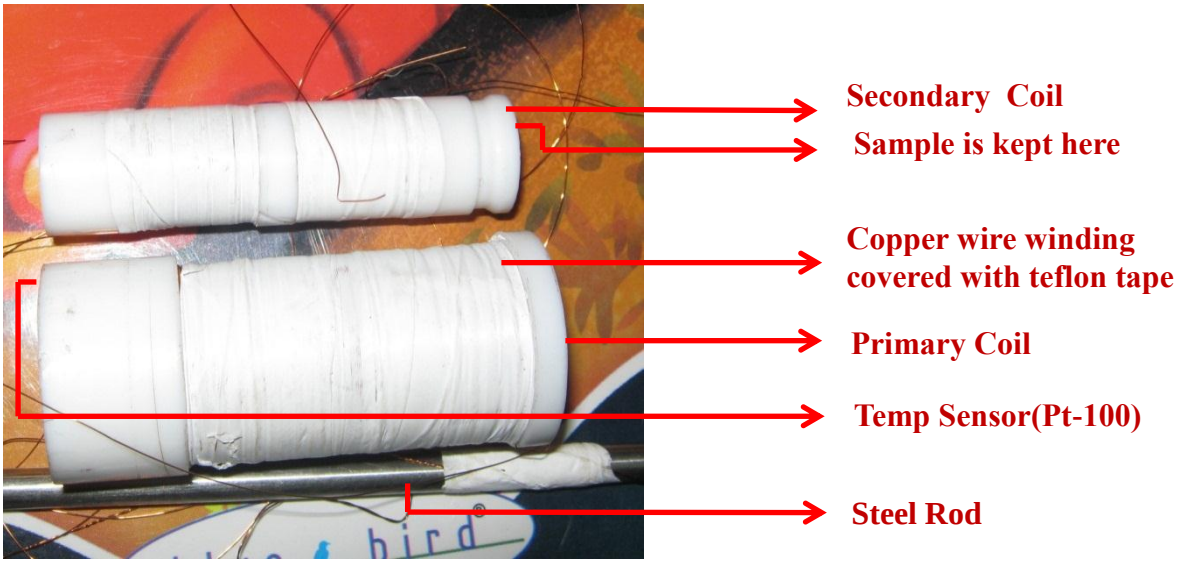

Figure-2.5 shows the primary and secondary (after winding) as per 2nd design

2.5 CALCULATION

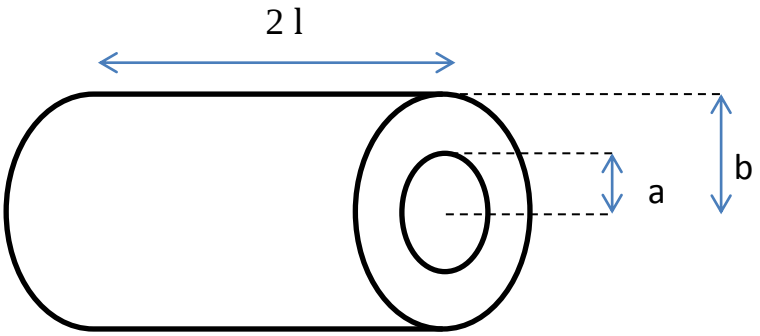

The magnetic field at the centre of the solenoid is given by :-

$$H = \mu_0 J a F(\alpha, \beta) \qquad (1)$$

where $F(\alpha, \beta)$ is the field factor which depends on the cross-sectional shape of solenoid.

$$F(\alpha, \beta) = \beta ln \left\{ \frac{\alpha + \sqrt{(\alpha^2 + \beta^2)}}{1 + \sqrt{(1 + \beta^2)}} \right\}$$

where $\alpha = b/a$

$$\beta = l/a$$

For the set-up we have designed, the value of $a = 7.5mm$, $b = 12.5mm$ and $l = 20mm$

Putting these values we get, $\alpha = 1.67$ and $\beta = 1.33$. So, the value of $F(\alpha,\beta)$ comes to

$$F(\alpha, \beta) = 0.59$$

The calculated amount of current passing through the solenoid is $I = 5\ \mu A$

So, the average current density $J = I/A$

$$A = 2l(b - a) = 200 * 10^{-6}$$

The value of J comes to $J = 0.25\ A/m^2$

So, $H_{ac} = 13.89$ Tesla

The measured rms voltage V across the two secondary coil is :-

$$V(t) = -d\emptyset/dt$$

The magnetic flux through the N turn oppositely wound coils of radius a is :-

$$\emptyset = \pi a^2 N M(t) \mu_0$$

With M(t) denoting the magnetic induction inside the sample averaged over the volume V.

So, $$V(t) = -\mu_0 \pi a^2 N dM(t)/dt$$

But for complex susceptibility χ_n' and χ_n'' one can do a Fourier expansion of $M(t)$

$$M(t) = \sum H_{ac} (\chi_n' \cos n\omega t + \chi_n'' \sin n\omega t)$$

Putting $M(t)$ in the eq of V(t) ,we get,

$$V(t) = V_0 \sum n(\chi_n' \sin n\omega t - \chi_n'' \cos n\omega t)$$

Where $V_0 = \mu_0 \pi a^2 \omega N H_{ac}$

$$V_0 = 4\pi \times 10^{-7} \times \pi (7.5 \times 10^{-3})^2 \times 2\pi \times 843 \times 1000 \times 13.89$$

$$V_0 = 2.46 \times 10^{-2} \text{ Volts.}$$

The real and imaginary component of susceptibility χ_n' and χ_n'' are determined from the relation,

$$\chi_n' \sin n\omega t = \frac{V(t)}{nV_0}$$

$$\chi_n'' \cos n\omega t = \frac{V(t)}{nV_0}$$

Here H is alternating magnetic field $H(t) = H\cos(n\omega t)$. n=1 denotes the fundamental susceptibility while n= 2,3,4… etc are the higher order harmonics associated with non linear terms in χ . Hence the signal which is in-phase $(n\omega t = 0)$ with the input signal gives χ_n', while 90^0 out-of-phase $(n\omega t = 90)$ signal with respect to the input gives χ_n''.

CHAPTER 3

SAMPLE PREPARATION

3.1 CHOICE OF SAMPLE

There are various reasons which account for the selection of Cobalt ferrite, a ferrimagnetic ceramic. They are enumerated below:-

1. Magnetic ferrite nanoparticles (commonly called ferrofluids) have been widely used in various applications, such as
   (i) Smart seal magnetic circuits
   (ii) Audio speakers
   (iii) Magnetic domain detectors

Figure-3.1 shows $CoFe_2O_4$ as ferrofluid with spikes when brought near magnet.[12]

Recently, magnetic nanoparticles have been suggested for many new applications in

(i) High density magnetic data storage.
(ii) Magnetic resonance imaging.
(iii) Catalyst supporters.
(iv) Biomedical applications such as magnetic carriers for bio-separation, enzyme and protein immobilization.

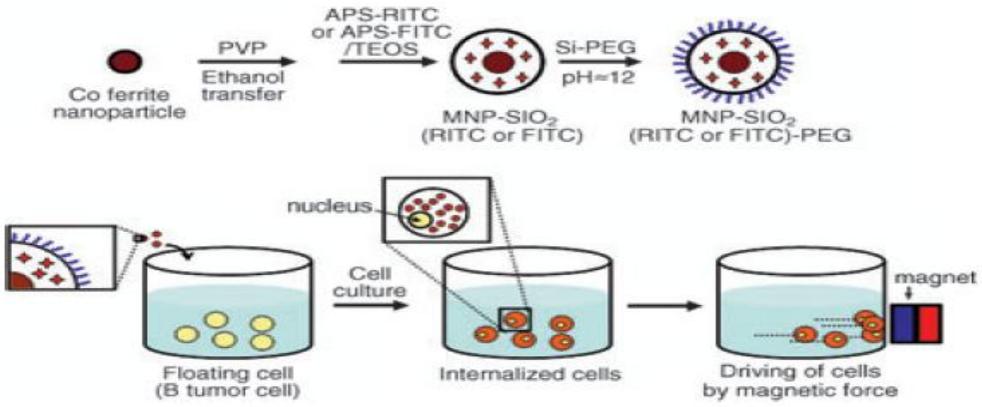

Figure-3.2 shows $CoFe_2O_4$ application in bio-medical for treatment of tumor cells.[12]

2. Spin valves requires that moment of one of the ferromagnetic layers be fixed in a specific direction or "pinned" which is accomplished by exchange anisotropy.$CoFe_2O_4$ has the highest anisotropy constant of the cubic ferrite due to trigonal distortion of the lattice. Hence they find application in spin valves.

3. $CoFe_2O_4$ is a very promising candidate for room temperature spin filter application because of its high Curie temperature(T_c =793K) and good insulating properties.

   Spin filter involves the spin selective transport of electrons across a magnetic tunnel barrier. Spin filtering could potentially impact future generations of spin –based device technology not only because spin filters function with 100 % efficiency. Moreover they combine with non-magnetic metallic electrode to provide a versatile alternative to half metals.

   Electronic band structure calculation methods predicts $CoFe_2O_4$ to have a band gap of 0.8eV and exchange splitting of 1.28eV between the minority (low energy) and majority (high energy) levels in the conduction band, thus confirming its potential to be a very efficient spin filter.

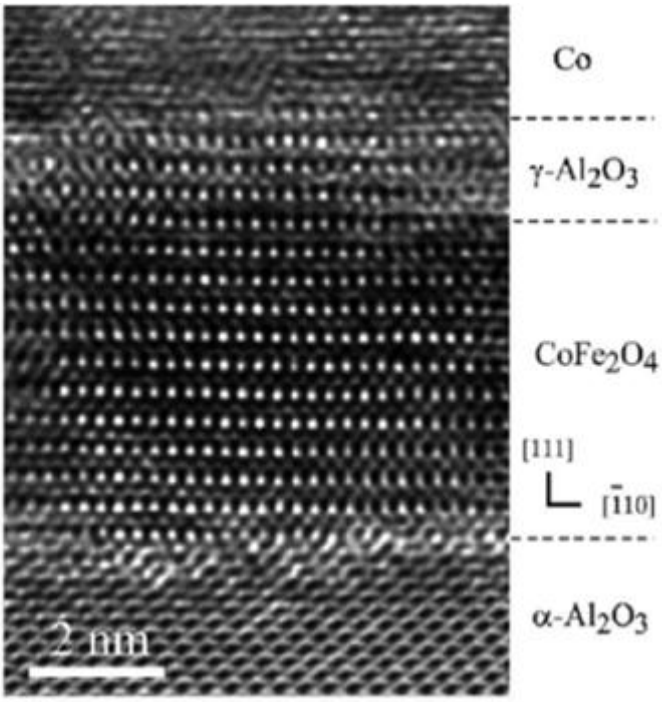

Figure-3.3 shows the HRTEM image of $CoFe_2O_4$(5nm)/γAl_2O_3 (1.5nm)/Co(10nm) trilayer having application in spin filtering.[13]

4. Use of $CoFe_2O_4$ bulk powder as anode material in lithium-ion batteries.

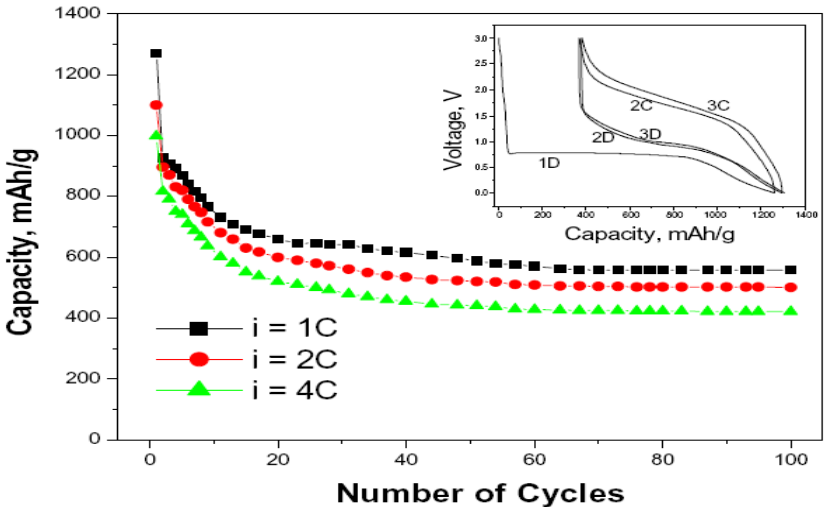

Figure- 3.3 shows $CoFe_2O_4$ film electrode cycled between 3.0V and 0.01V at different rates. The current carrying capacity of lithium-ion battery for different cycles. [14]

5. Spinel type ferrites MFe_2O_4 (M=Co, Ni) are among the most important magnetic materials. Special magnetic and electrical properties, high chemical and mechanical hardness in modern information technology have made ferrite films

significantly important while designing the electro-magnetic devices including the memories, sensors and microwaves.

6. On account of large magnetocrystalline anisotropy high coercivity, moderate saturation magnetization, large magnetostictive co-efficient , chemical stability and mechanical hardness which generally are useful for magnetic recording and electronic devices $CoFe_2O_4$ are nowadays highly in demand.

7. Wavelength-dependent magneto-optical coercivity in cobalt ferrite nanoparticles

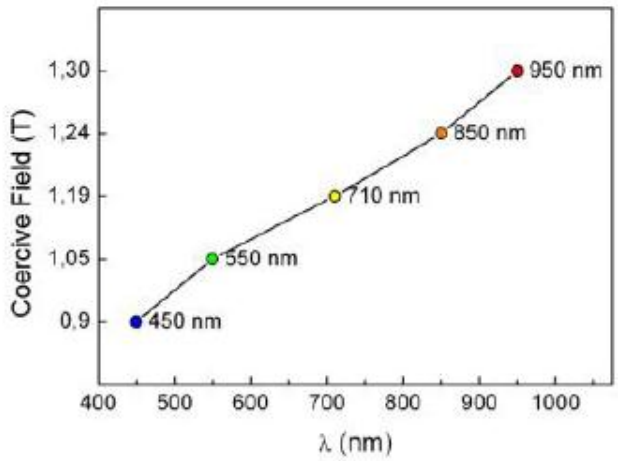

Figure-3.4. shows the wavelength dependent coercivity of $CoFe_2O_4$.[15]

8. $CoFe_2O_4$ has direct implication in hydrogen production .Water splitting process can produce H_2 gas , which is a promising solar fuel and has the advantage that H_2 and O_2 gases can be separately recovered due to the two separated steps of H_2 generation step and O_2 releasing step.The two step water splitting processor can be presented as:-

O_2 generation,

$xMO(ox) + \text{solar energy} \rightarrow xMO(red) + 1/2O_2$

H_2 generation,

$1/2MO(red) + H_2O \rightarrow xMO(ox) + H_2$.

MO(red) and MO(ox)denote the reduced and oxidized state respectively. The net reaction is

H_2O +solar energy $\rightarrow$ H_2 +1/2O_2

Iron oxide have high possibility for utilization in the two step water splitting system as they are oxides with different oxidation states.

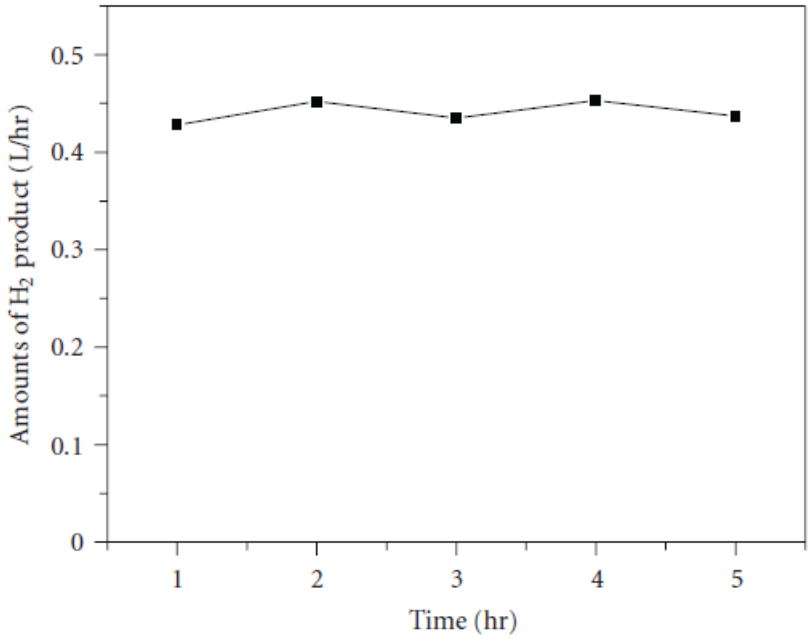

Figure-3.5 shows the quantitative measurement of hydrogen production rate using $CoFe_2O_4$. **[16]**

9. Due to very high specific resistance, remarkable flexibility in tailoring the magnetic properties , ease of preparation , price and performance considerations make ferrites the first choice materials for microwaves applications. The most important microwave device, utilizing the non-reciprocity of ferrites, is the circulator. A typical use of the circulator is in communication (radar, mobile phone) equipment where it enables the radar transmitter to use the same device for transmission and receiving.

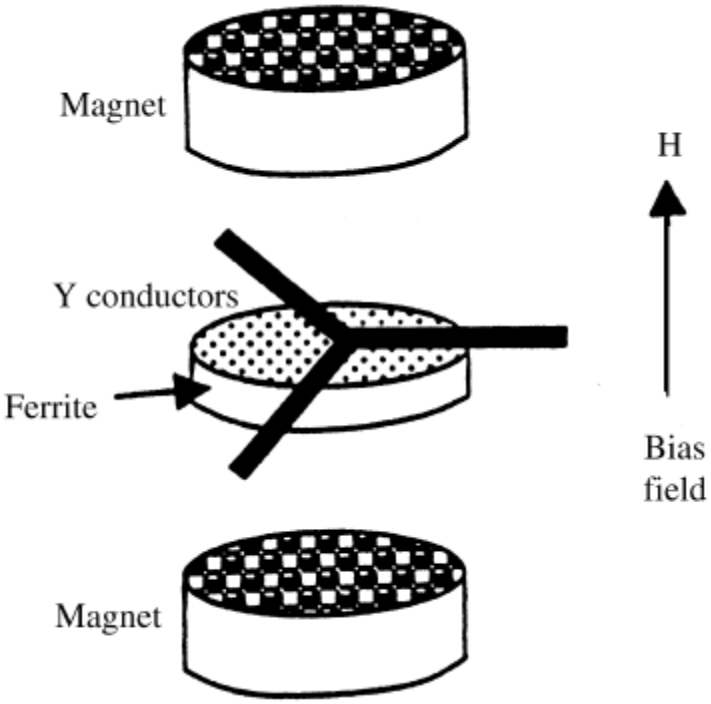

Figure-3.6 shows circulators,a microwave device which is made of ferrite material [17]

10. $CoFe_2O_4$ based magnetostrictive materials are effective for use as magnetic stress sensors and actuators applications.

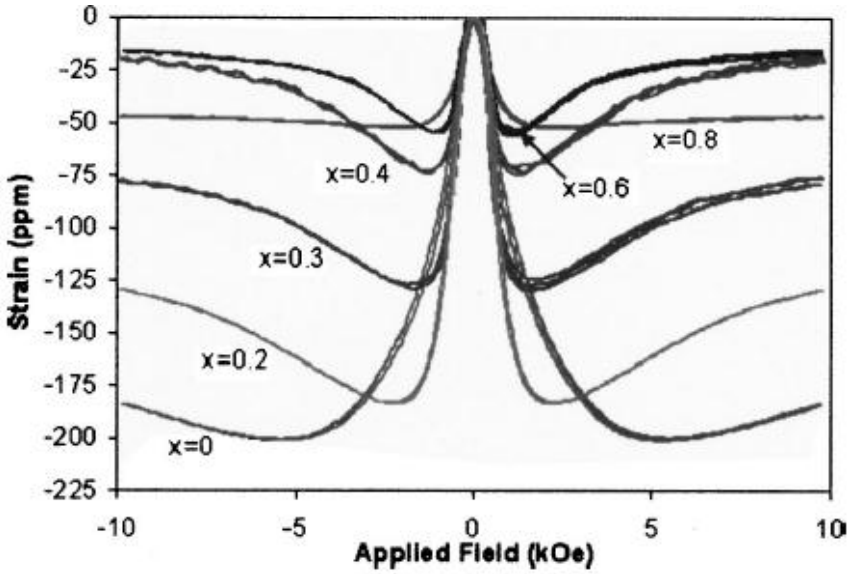

Figure-3.7 shows Strain Vs applied field magnetostriction curves of $CoFe_{2-x}Mn_xO_4$.[18]

3.2 REVIEW OF SYNTHESIS TECHNIQUES.

There are various methods employed for the preparation of $CoFe_2O_4$. $CoFe_2O_4$ can be synthesized in various forms like bulk , nanoparticles ,thin films etc. There are broadly two methods of preparing the magnetic nanoparticles.

- Physical Method .
- Chemical Method .

The former is based on the *top down* approach which involves breaking down of bulk particle of μm order into nano dimensions. They are then ball milled to get the desired size. In contrast, the later uses the *bottom up* approach in which building of nanoparticles occur from particles much smaller than nano(may be pico etc.).

From the literature survey it was observed that there are numerous methods of preparation of $CoFe_2O_4$,of which some are :-

- ✓ Sol-gel Route [19]
- ✓ Synthesis in microemulsion [20]
- ✓ Citrate Precursor Method [21]
- ✓ Mechanically alloyed $CoFe_2O_4$ after heat treatment Method [22]
- ✓ Auto Combustion Sol-gel Method [23] .etc.

In the sol-gel method the starting materials were iron nitrate, aluminium nitrate, cobalt nitrate, citric acid and ammonia. In the combustion method appropriate ratio of iron nitrate and cobalt nitrate and glycine were dissolved in deionized water. The sol-gel derived nanosized cobalt ferrite can be synthesized by sol-gel combustion method, the fuel used is ethylene glycol. In the methods mentioned above, there are various fuels used like Glycine [23] ,Citric Acid [19] ,ethylene glycol [24] etc.

3.3 EXPERIMENT

Nanophased $CoFe_2O_4$ Prepared By Combustion Method.

This is a very simple method of synthesis. The precursor used here are $Fe(NO_3)_3.9H_2O$, $Co(NO_3)_2.6H_2O$ and glycine (NH_2CH_2COOH) as the chelating agent. The molar concentration of $Fe(NO_3)_3.9H_2O$ and $Co(NO_3)_2.6H_2O$ was taken to be 0.02 mole and mass was 8.08 gm and 5.8208 gm respectively. The ratio of metal nitrate : glycine was maintained to 1:1.So, the mass of glycine came to be 3.0028 gm.

$Fe(NO_3)_3.9H_2O$ was dissolved in 25 ml distilled water and a saffron colour solution was obtained. Again $Co(NO_3)_2.6H_2O$ was dissolved in 25 ml distilled water , a brick red (pinkish) colour solution was obtained . A 500ml beaker was taken and the measured amount of glycine was added to it .Then both the precursor solution were pour into it and a magnetic stirrer was kept in it. The beaker was then kept on a magnetic heater and the excess water was allowed to evaporate. The solution got converted into gel and finally the combustion reaction started which resulted in black porous ash filling the container. The ash-burnt powder was ground and calcined at temperature of 600^0 C for 2 hours with a heating rate of 5^0C /min to obtain the spinel phase. After cooling , the sample was collected from the furnace and again ground in the agate mortar. The sample was then pressed in pellet in the hydraulic press and then sintered for 5h at 825^0C.

The structural characterization of the prepared Cobalt Ferrite was carried out by X-ray Diffraction technique(XRD) , the scan range was 20^0 to 80^0 and formation of well-defined single phase spinel structure was confirmed.

3.4 FLOWCHART

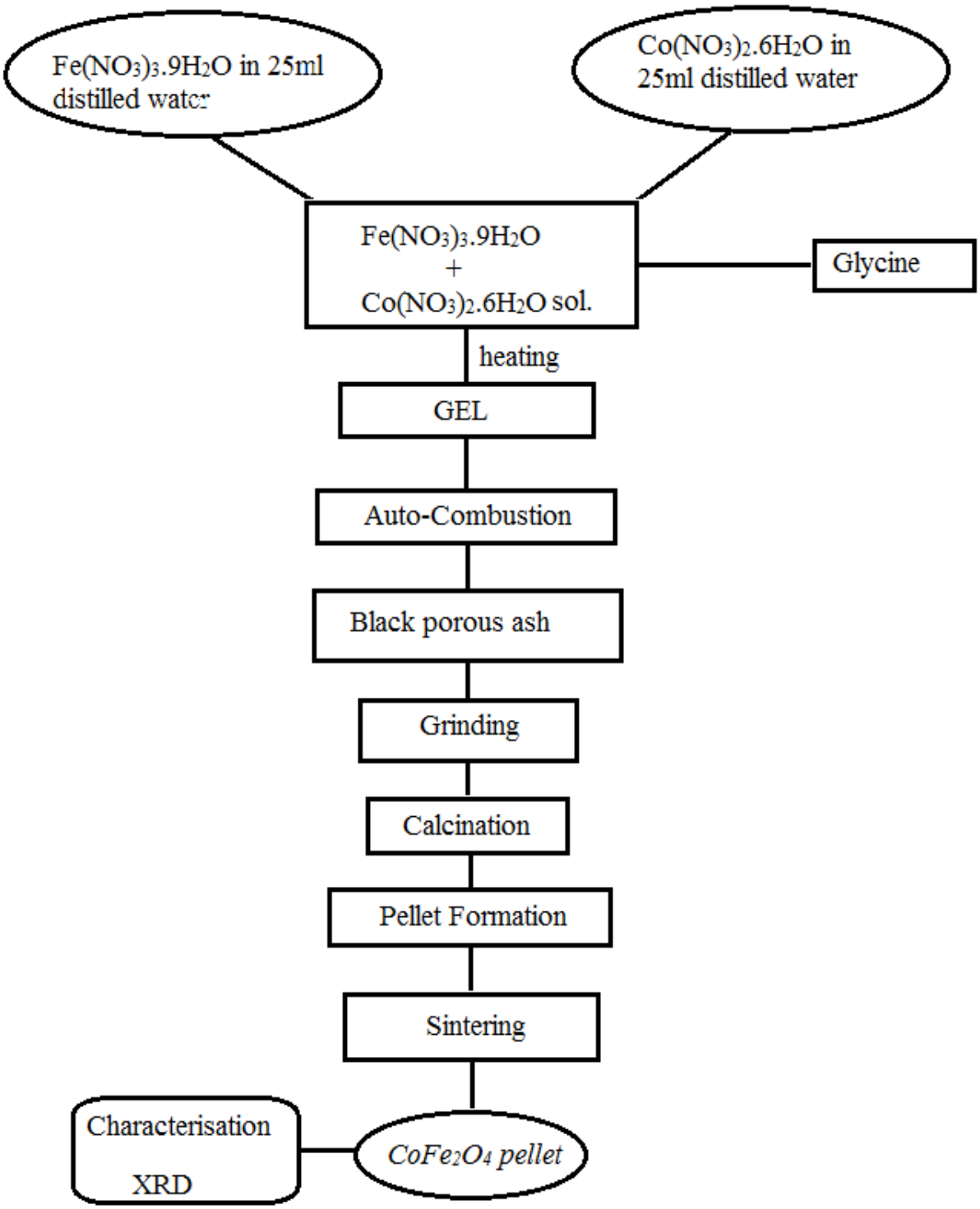

Flowchart for the preparation of Cobalt Ferrite by auto-combustion method.

CHAPTER-4

RESULTS AND DISCUSSION

4.1 XRD ANALYSIS OF $CoFe_2O_4$.

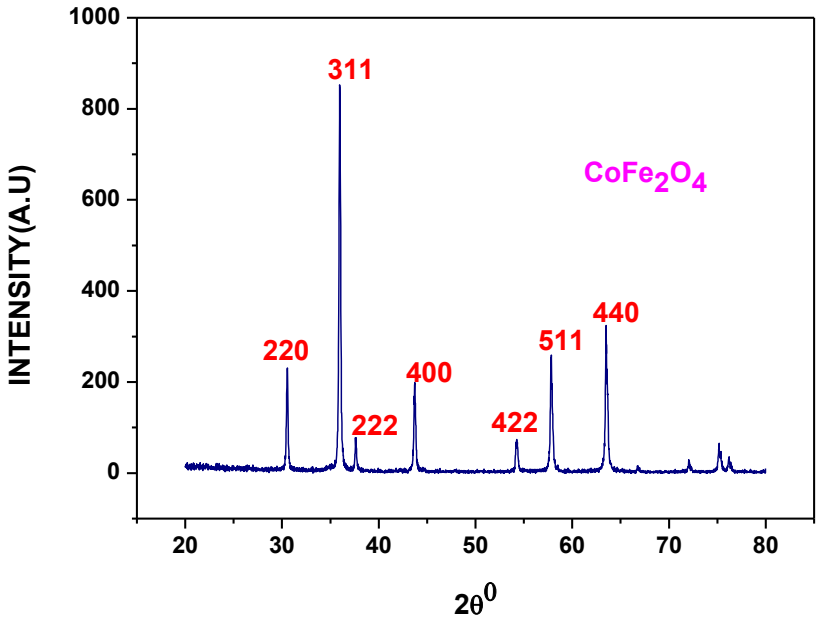

Figure-4.1 shows the XRD graph of CFO.

The structural characterization of the sample was carried out by XRD technique. The above graph is in good agreement with the standard one. So, it was confirmed that the sample was prepared properly. The crystallite size is calculated using the **Scherrer formula**.

$$t = \frac{0.9\lambda}{\beta \cos\theta}$$

The FWHM and the 2θ values were calculated using a standard software ***"Peakfit"***.

FWHM = β = 0.00341 radian and 2θ = 17.9857radian

So, $t = 42.791319\ nm$

Hence, we conclude the prepared sample of $CoFe_2O_4$ is of nano-size order. Therefore, $CoFe_2O_4$ is also called as magnetic nano particle (MNP).

4.2 HIGH TEMPERATURE MEASUREMENT

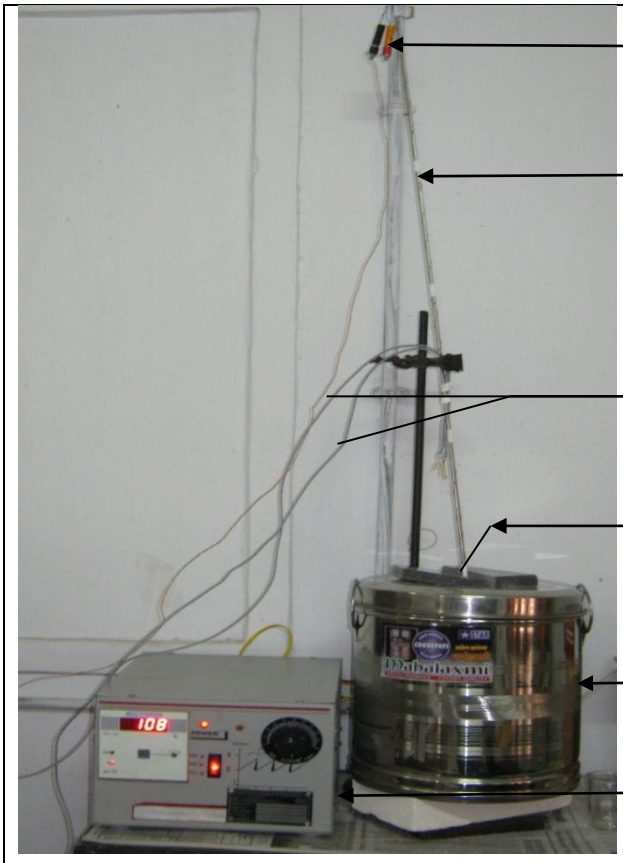

Figure-4.2 shows high temperature setup.

Figure-4.3 shows multimeter and lock-in amplifier.

Now the setup and the sample both are ready for susceptibility measurement. The two terminals of the secondary coil are connected to the input of the lock-in amplifier and the

primary coil with the lock-in output. The temperature sensor which was put in a hole in the setup was connected to a multimeter.

For high temperature susceptibility measurement, the whole setup was placed inside a furnace and empty run was carried out. The data was recorded for heating up to 184^0C as well as cooling process.Then measurements were done with sample.

4.3 AC SUSCEPTIBILITY OF $CoFe_2O_4$ (CFO).

The $CoFe_2O_4$ sample pellet was cut into cylindrical shape. This cut sample was then wrapped in teflon tape to get the desired thickness so that it penetrates into the secondary coil tightly. The sample was cautiously placed in the outer coil of the secondary coil. The sample is adjusted in such a way that it is in the middle of outer secondary coil. The temperature of the furnace was controlled by a temperature controller attached to it. The multimeter showed the resistivity value which was later converted to temperature. The data was recorded for the heating upto 184^0C as well as cooling process. This gives us the background plus sample data. To get the sample readings both the readings i.e, with sample and without sample were subtracted. The lock-in amplifier gave the in phase and out of phase voltages V_x and V_y .To convert it into susceptibility, it was divided by V_0 [25]. Plot of Susceptibility (real part **χ'** and imaginary part **χ"**) Versus Temperature was done using standard software ***"Origin"***.

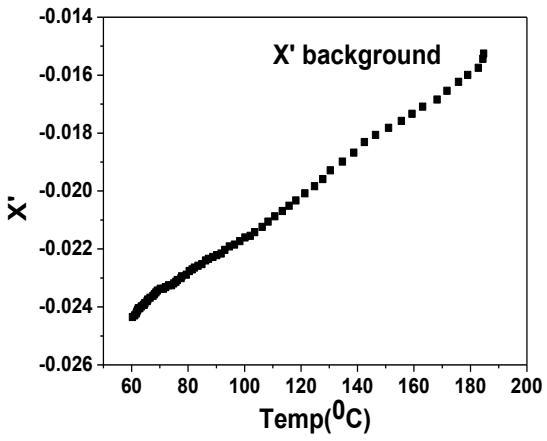

Figure-4.4 is the plot of the susceptibility χ'(in phase) Vs Temp (^{0}C) of the background.

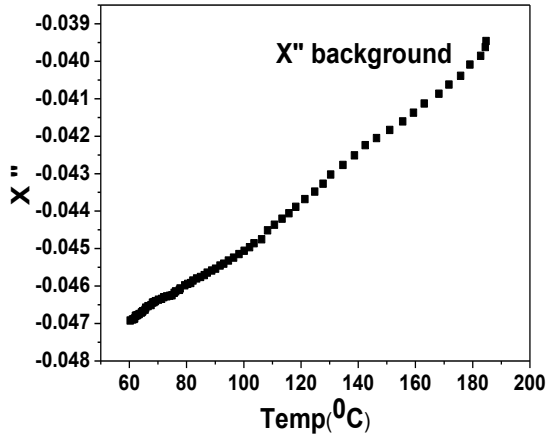

Figure-4.4 is the plot of susceptibility χ"(out of phase) Vs Temp (^{0}C) of the background.

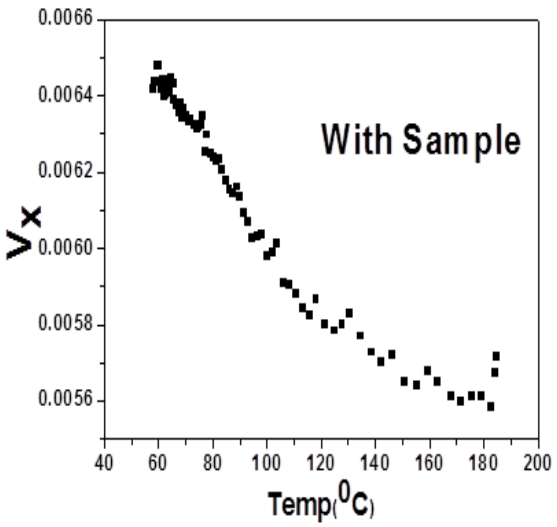

Figure-4.5 shows the V_x Vs tempresponse of the background and sample together.

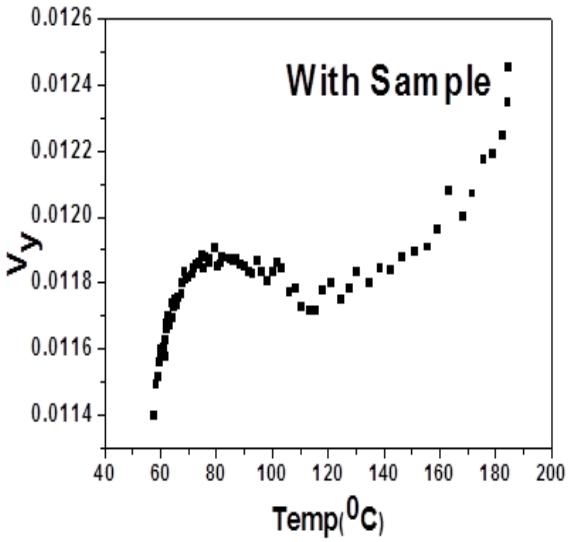

Figure-4.6 shows the V_x Vs temp response of the background and sample together.

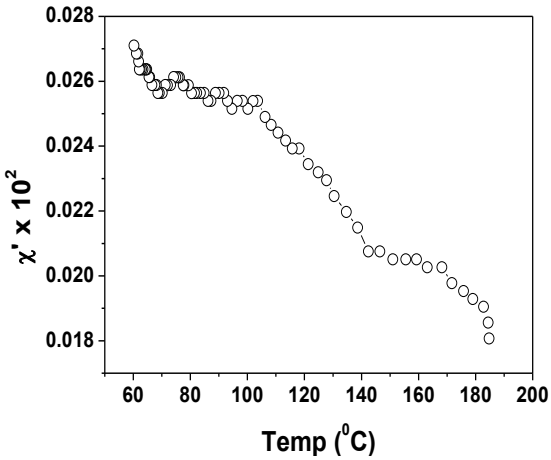

Figure-4.7 shows the plot of Susceptibility(χ') Vs Temp response of the sample.

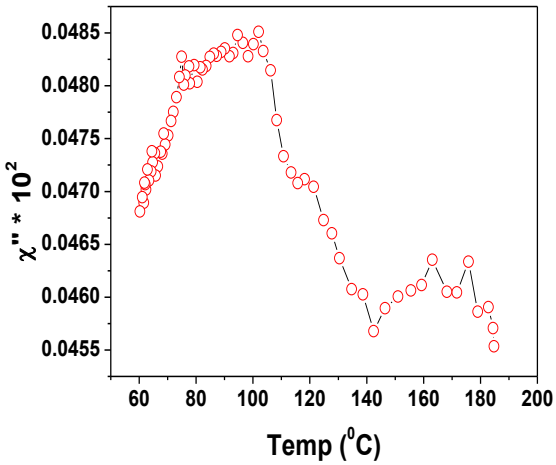

Figure-4.8 shows the plot of susceptibility(χ") Vs Temp response of the sample.

The standard plot of χ' with temperature is given in figure below.The transition temperature of CFO is very high around 793 K so the transition is not shown here.The figure shows decreasing trend of susceptibity with temperature.This nature is very well shown in our case.

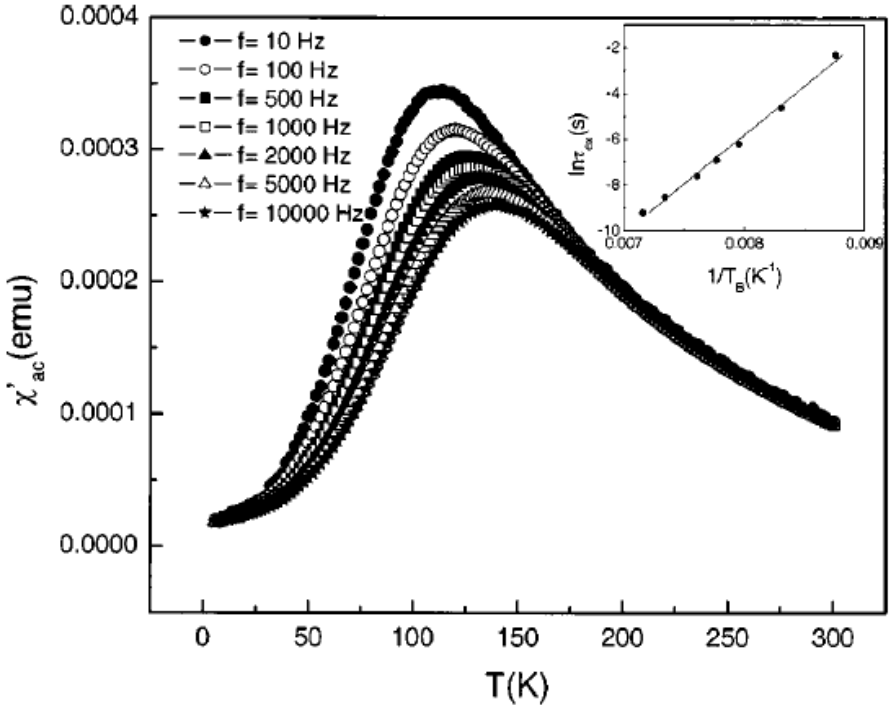

***Figure-4.9 shows the standard in phase component of ac susceptibility at different frequencies within 300K.*[26]**

CHAPTER – 5

CONCLUSION

This project involves the fabrication of susceptometer. A design of susceptometer was prepared and then its fabrication part was carried out. The setup was so designed that it consisted of three parts i.e, the primary coil, secondary coil and sample holder. Copper wire winding was done of the secondary and primary coil. The material chosen was Teflon as it has a high melting point of ~600 K.

Then sample was prepared for its susceptibility measurement. The sample chosen was Cobalt Ferrite ($CoFe_2O_4$), a ferromagnetic material for high signal. The sample was prepared by auto combustion sol-gel method. For the combustion purpose the fuel used was glycine. The XRD analysis of the sample was carried out. The crystallite size of the sample was calculated, which comes to be 42.79 nm CFO. The graph obtained by XRD analysis matches with that of the standard graph. No extra peaks were formed indicating the sample is in single phase.

The sample was inserted in the sample holder part of the fabricated susceptometer. For high temperature measurement when the sample was inserted in the furnace, it got melted. As the vendor had supplied us with wrong material. Unfortunately, we lost the setup and the prepared sample all together.

Then again a new design was made with some modifications. This time the sample holder part was omitted. The sample was instead placed in the secondary coil so that there is high induction. The secondary coil is then inserted in the primary. The sample was also again prepared. After all the connections of the setup are made with the lock-in amplifier and multimeter, the measurement was done. Firstly at room temperature and then at high temperature of around 200^0 C. Then the graphs were plotted and the results were carried out.

The plotted graphs very well matched with the standard one indicating proper working of our setup .

APPENDIX

This is a collaborative project with Debjani Banerjee. We have fabricated a single set-up but two samples were prepared separately. Cobalt Ferrite and Lanthanum Strontium Manganite (LSMO) were prepared. The XRD characterization of both the samples were carried out. The detailed case of $CoFe_2O_4$ is explained in this thesis and the elaborate discussion of LSMO can be found from the thesis of Debjani Banerjee. The brief discussion of her results are given below.

XRD ANALYSIS OF LSMO

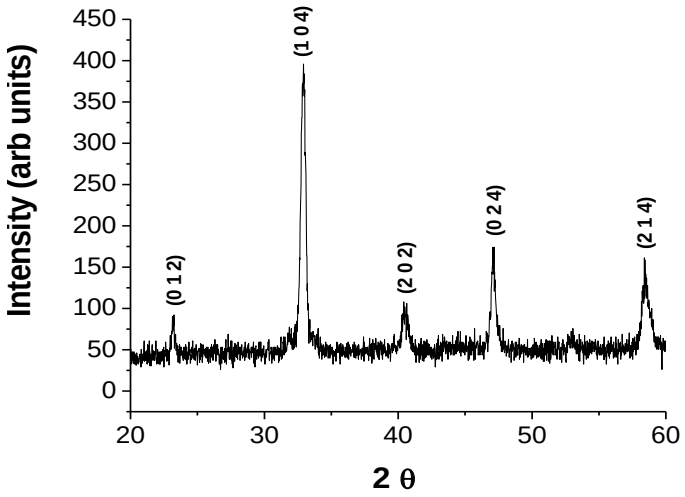

The crystallite size was calculated using the Williamson Hall method. The crystallite size came to be 81.5 nm.

The high temperature measurement plot of susceptibility and temperature are given in the next page.

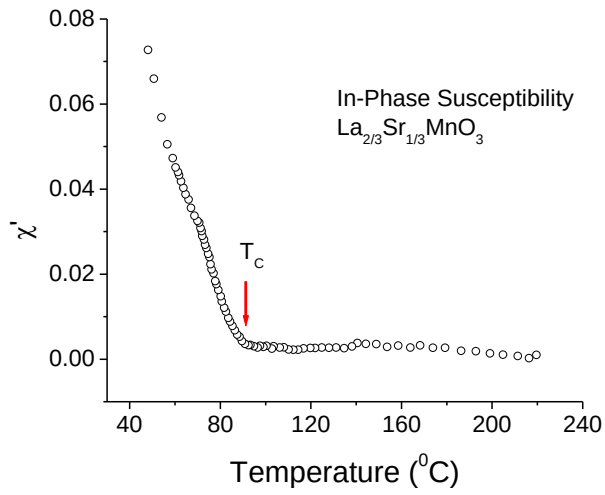

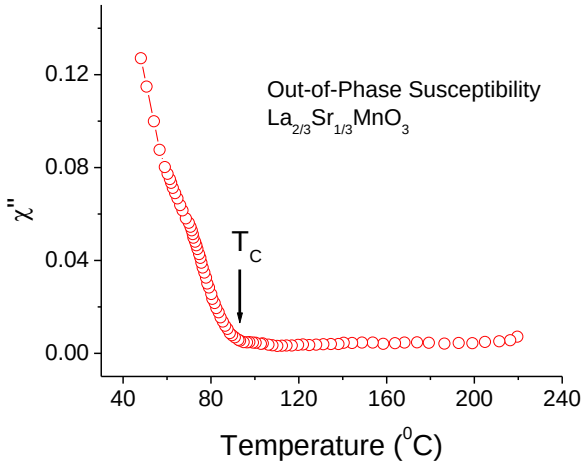

Figure shows the in phase susceptibility Vs temp. at high temp.measurement

Figure shows the out of phase susceptibility Vs temp. at high temp.measurement

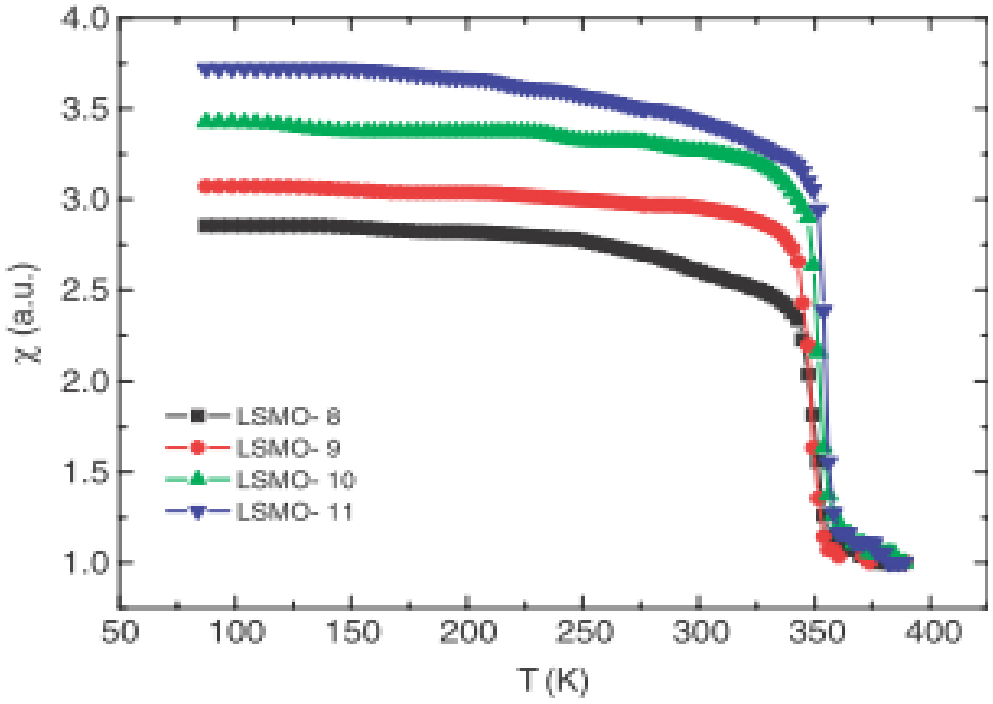

Figure shows the standard transition plot of LSMO .

From literature we get the transition temperature of LSMO is 364K i.e at this temperature it changes from ferromagnet to paramagnet. This standard value is very much in good agreement with the value above plotted figure by her.

REFERENCE

[1] B.D. Cullity and C.D.Graham,Introduction to magnetic materials,IEEE Press WILEY Publication (2009).

[2] Charles Kittel , Introduction to Solid State Physics, WILEY Publication.

[3] Rev. Sci. Instrum.,**30**,548(1959).

[4] www.hyperphysics.phy-astr.gsu.edu

[5] K. Binder and A.P. Young,Rev. Mod. Phy s.,**58**,801(1986).

[6] Joel S. Miller,Marc Drillon,Magnetism : Nanosized magnetic materials WILEY-VCH(2002).

[7] Robert A. Hein, Thomas L Francavilla,D.H. Liebenberg,Magnetic Susceptibility of superconductors and other spin system,Springer(1999).

[8] M. I. Youssif et.al., [Egypt. J. Sol., 23, 231(2000)].

[9] M. Nikolo et al., Am. J. Phys. 63, 57 (1995).

[10] A.Charavorothy, R.Ranganathan and A.K.Raychaudhuri, Pramana et al., **36**, 231 (1991).

[11] S. Kundu & T.K.Nath, J. Magn.Magn. Mater, 322, 2408(2010) .

[12] Tae-Jong Yoon et al.,Angew .Chem . Int.Ed.2005,**44**,1068-1071.

[13] A.V.Ramos et al., Applied Physics Letters **91**,122107(2007).

[14] Yan Qiu Chu et al., Electrochi mica Acta **49**(2004) 4915-4921.

[15] Pineider et.al. Università di Firenze & INSTM, Italy 2. Università di Padova & ISTM-CNR, Italy.

[16] Gaikwad et al., International Journal of Electrochemistry,Volume 2011 ,Article ID 729141 (2011).

[17] Horvath et al., Journal of Magnetism and Magnetic Materials 215-216(2000) 171-183.

[18] Paulson et al., Journal of Applied Physics **97** ,044502 (2005).

[19] Gul *et al.*,Journal of Alloys and Compounds **465**(2008) 227-231.

[20] Mathew *et al.*, Chemical Engineering Journal **129** (2007) 51-65.

[21] Verma *et al.*, Journal of Magnetism and Magnetic Materials **208**(2000) 13-19.

[22] Ding *et al.*, Solid State Communications,Vol. **95**,No. 1, pp. 31-33, 1995.

[23] Yan *et al.*,Solid State Communication **111** (1999) 287-291.

[24] Gopalan *et al.*,Journal of Alloys and Compounds **485**(2009) 711-717.

[25] Nikolo *et al.*, Physics Department , St. Louis University, St Louis, Missouri 63103

(Revised 23 February; accepted 20 June 1994).

[26] L. D. Tung, V. Kolesnichenko, D. Caruntu, N. H. Chou, C. J. O'Connor, and L. Spinu, J. Appl. Phys., **93**, 7487 (2003)